ACS OMEGA

http://pubs.acs.org/journal/acsodf

Article

Insight into the Loading Properties of Na^+ Green-Functionalized Clinoptilolite as a Potential Carrier for the 5-Fluorouracil Drug, its Release Kinetics, and Cytotoxicity

Mohamed Adel Sayed, Hayam M. El-Zeiny, Jong Seong Khim, Jamaan S. Ajarem, Ahmed A. Allam, and Mostafa R. Abukhadra*

Cite This: *ACS Omega* 2022, 7, 6991−7001

Read Online

ACCESS | Metrics & More | Article Recommendations | Supporting Information

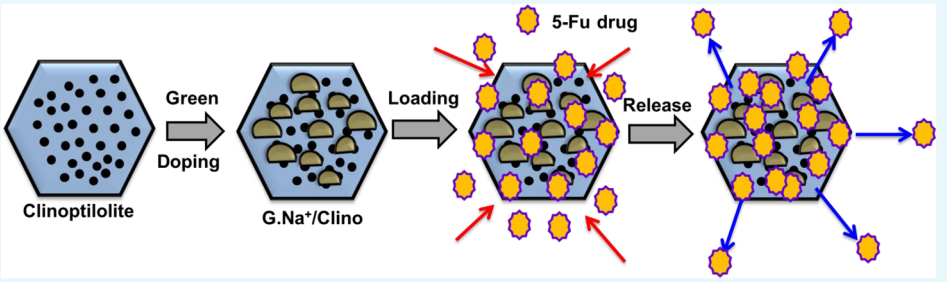

ABSTRACT: Herein, natural zeolite (clinoptilolite) was functionalized by Na^+ ions ($G.Na^+$/Clino) utilizing a green tea extract prepared by a green production method as a potential carrier for the 5-fluorouracil (5-Fu) drug with enhanced physicochemical behaviors. The $G.Na^+$/Clino-modified product showed enhanced surface area (312 m^2/g) and ion-exchange capacity (387 mequiv/100 g). The loading studies reflect high and controlled loading properties of $G.Na^+$/Clino with an actual loading capacity of 291 and 462 mg/g, respectively. The loading reactions of 5-Fu into $G.Na^+$/Clino were of pseudo-second-order kinetics and exhibited Langmuir isotherm properties. This suggested a monolayer and homogeneous loading process by chemical complexation and ion-exchange mechanisms with a Gaussian energy value of 10.47 kJ/mol. Additionally, these reactions were of endothermic and spontaneous nature based on the determined thermodynamic parameters. The release studies demonstrated the 5-Fu release profile for about 150 h at pH 1.2 and for 80 h at pH 7.4. The release reactions had non-Fickian transport properties and were controlled by both erosion and diffusion mechanisms, considering the release kinetic findings and the values of the diffusion exponent (0.42 at pH 1.2 and 0.37 at pH 7.4). The composite showed remarkable biocompatibility based on the measured cell viability and a cytotoxic effect on normal colorectal cells (CCD-18Co). Additionally, the application of $G.Na^+$/Clino as an inorganic carrier for the 5-Fu drug prompted the cytotoxic effect of the drug on colon cancer cell treatment (HCT-116).

1. INTRODUCTION

About 71% of worldwide deaths are ascribed to non-contagious diseases that are related to physiological, genetic, and environmental factors.[1] From the previous reasons, cancer can be listed as the second main cause of worldwide deaths.[2] Based on the recent expectations, the world will face grave challenges of an interminable increase of cancer deaths by 75%, especially from colorectal cancer (CRC).[3] CRC is extensively distributed in the world, especially in developing and poor countries.[4] This directed the interested researchers and health authorities to introduce and develop innovative, efficient, low-cost, and safe therapies to be suitable for such poor countries.[5,6] Additionally, great efforts have been made to enhance the performance of common chemotherapeutic drugs such as 5-fluorouracil (5-Fu), considering the bioavailability, efficiency, solubility, and specificity of the drug toward tumors.[2,4,7]

Although the 5-Fu drug is an efficient chemotherapeutic drug for several species of cancers such as breast, rectal, and stomach cancers, its use is accompanied by some significant drawbacks.[1,8] This is related to its low selectivity, limited solubility, high diffusion rate, and toxic properties of 5-Fu overdosage.[7,9] This resulted in an increment in the required dosage during the treatment periods which might cause damage to the uninfected cells. Additionally, such high dosages exert toxic effects on the gastrointestinal tract, nervous system, hematological system, cardiac system, and cause dermato-

Received: November 24, 2021
Accepted: February 1, 2022
Published: February 15, 2022

https://doi.org/10.1021/acsomega.1c06671
ACS Omega 2022, 7, 6991−7001

logical reactions.[8,9] Therefore, introducing appropriate carriers or delivery systems for the 5-Fu drug molecule has insistent demand to overcome the common technical and health side effects.[1,10]

The developed carriers or 5-Fu delivery systems were designed to deliver the drug at a controlled diffusion rate, certain dosages, and targeted pathways.[3,11] Moreover, the advanced carriers have a strong impact on inducing the solubility of the 5-Fu drug, the patient compliance, and the curative profiles, in addition to their role in reducing the drug degradation rate and preserving the concentration at the recommended therapeutic level.[12,13] Besides the previous requirements, the selection of the appropriate carrier depends mainly on the fabrication cost, biocompatibility, availability, loading capacity, release rate, and cytotoxicity of the material.[7,14,15] Therefore, numerous materials were introduced as effective carriers for 5-Fu drugs including natural zeolite;[4,16] biopolymers such as cellulose, alginate, and chitosan;[5,15] montmorillonite;[9] kaolinite;[8] and layered double hydroxide.[17]

The natural phases of zeolite such as clinoptilolite, phillipsite, and mordenite are from massive geological reserves and have a significantly low mining cost.[18,19] In addition to their low cost, such materials have many technical merits such as chemical stability, biocompatibility, non-toxicity, high surface area, remarkable ion-exchange capacity, and significant loading efficiency.[20,21] Moreover, such zeolitic phases exhibit a supportive effect on the immune activity in addition to their hemostatic, anti-diarrheal, and anti-oxidant properties.[22,23] Therefore, the different phases of natural zeolite can be used as potential drug carriers with promising loading capacity and enhanced release behavior.[24,25]

However, the surface modification, chemical functionalization, and decoration of zeolite minerals by nanoparticles play a significant role in enhancing their technical properties as adsorbents or delivery systems.[26] Recently, the green extracts of leaves and plants, as well as the enzymes, were applied as promising reducing, capping, and stabilizing bio-agents for the green modification of materials and the fabrication of non-agglomerated nanoparticles.[27,28] It is a low-cost technique, and the synthesized materials are environmental products with high surface area, reactivity, and biodegradability.[4] Our previous study demonstrated the significant role of the green modification of natural clinoptilolite in enhancing its morphology, surface area, reactivity, ion-exchange capacity, adsorption capacity, and environmental value.[29,30]

Herein, this study aimed to figure out the effect of the green Na^+ functionalization process on the technical properties of natural clinoptilolite (G.Na^+/Clino) as a potential delivery system for the 5-Fu drug possessing enhanced cytotoxicity, release, and loading behaviors. The study involved a detailed investigation of the effect of the loading parameters, the loading mechanisms, the release profile, the release kinetic properties, and cytotoxicity.

2. RESULTS AND DISCUSSION

2.1. Characterization of the Carrier. The zeolite structure shows numerous XRD peaks at 9.88, 11.18, 13, 14.9, 17.36, 17.5, 22.36, 22.7, 26, 26.87, 30, 32, 32.9, and 34°, which distinguish the natural clinoptilolite species (Figure 1A). After the green functionalization of clinoptilolite with Na^+ ions, the observed pattern shows a deviation in the essential peaks of zeolite (29.97, 25.56, and 22.35°) and the formation of a new crystalline phase of sodium silicate (33.85, 31.84, and 19.1°)

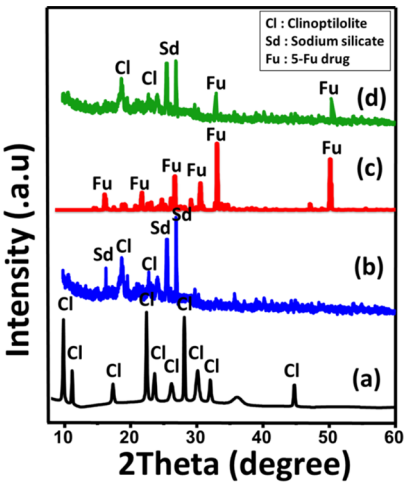

Figure 1. XRD patterns of raw clinoptilolite (A), green Na^+-functionalized clinoptilolite (G.Na^+/Clino) (B), free 5-Fu drug powder (C), and 5-Fu-loaded G.Na^+/Clino (D).

(JCPDS no. 16-0815) (Figure 1B). This reflected a significant effect of the process on the structure of zeolite by partial deformation and formation of new crystalline phases. Regarding the patterns of free 5-Fu (Figure 1C) and 5-Fu-loaded G.Na^+/Clino (Figure 1D), the reorganization of 5-Fu diffraction peaks in the pattern of 5-Fu-loaded G.Na^+/Clino confirmed the successful trapping of the drug molecules into the carrier (Figure 1D).

The impact of the modification process was studied for the chemical analysis of the products (Figure 2). The elemental

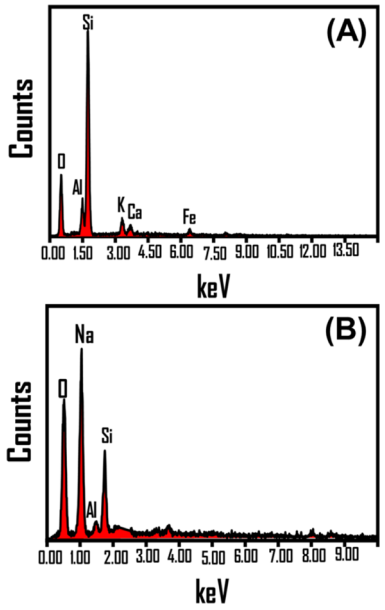

Figure 2. EDX spectra of raw clinoptilolite (A) and the synthetic G.Na^+/Clino composite (B).

composition of the precursor was found to be Al (7.21%), O (46.64%), Si (36.28%), Ca (1.98%), Fe (3.01%), and K (3.43%) (Figure 2A). After the modification step, the Na^+ content increased to 27.23%, while the structural Al and Si contents declined significantly down to 1.5 and 8.48%, respectively (Figure 2B). This confirms the successful trapping of Na^+ in the structure of clinoptilolite by partial substitution

https://doi.org/10.1021/acsomega.1c06671
ACS Omega 2022, 7, 6991−7001

or replacement processes with the structural Al and Si ions. The Si/Al ratio before (5.03) and after the modification step (5.65) reflected an increase in the hydrophobicity properties of G.Na$^+$/Clino. Therefore, it was expected that the modified sample (G.Na$^+$/Clino) will have a higher release rate for the hydrophilic 5-Fu drug.

The impact of such chemical changes on the structural active groups was studied by Fourier transform infrared (FT-IR) spectroscopy. The bands of the main zeolitic chemical groups were identified clearly in the spectra of both Clino and G.Na$^+$/Clino samples [O−T−O and/or T−O (T = Al and Si) (467 cm^{-1}), T−O bending (1041 cm^{-1}), zeolitic water (1640 cm^{-1}), and OH (4442 cm^{-1})][31] (Figure 3A,B). However, the

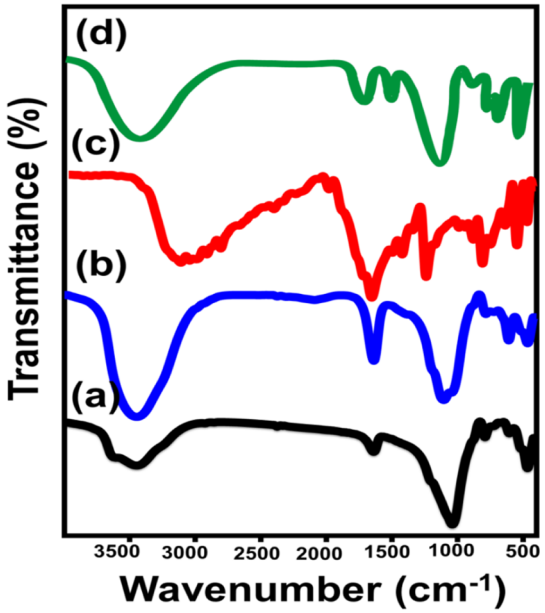

Figure 3. FT-IR spectra of raw clinoptilolite (A), synthetic G.Na$^+$/Clino composite (B), free 5-Fu drug powder (C), and 5-Fu-loaded G.Na$^+$/Clino (D).

spectrum of G.Na$^+$/Clino reflected significant intensification of the OH-related band. This signifies the role of the alkaline conditions in causing the etching and exposure of the siloxane and OH-bearing groups.[32] The spectrum of 5-Fu-loaded G.Na$^+$/Clino (Figure 3C) in comparison with that of the free 5-Fu drug (Figure 3D) showed some absorption bands related to the drug's chemical structure [CF═CH (485.3 cm^{-1}) and C═O (1780 cm^{-1})].[1] This confirms the entrapment of the 5-Fu molecules into the G.Na$^+$/Clino carrier.[33,34]

Regarding the morphological features, the Clino precursor showed aggregates of stacked flaky grains (Figure 4A). After the modification reaction, the G.Na$^+$/Clino particles were converted into highly ordered bunches that contained numerous nanoclusters of spherical or globular grains (Figure 4B−D). Therefore, the green functionalization process had an enhanced impact on the chemical and morphological properties of clinoptilolite and in turn on the textural and physicochemical properties. Considering the particle size of the raw zeolite (4−6 μm) and synthetic G.Na$^+$/Clino (100 nm to 0.5 μm), the observed reduction in the particles size is related to the change in the morphology, new phase of sodium silicate, and impact of the ultrasonic waves on the disintegration and dispersion of agglomerated zeolite particles.

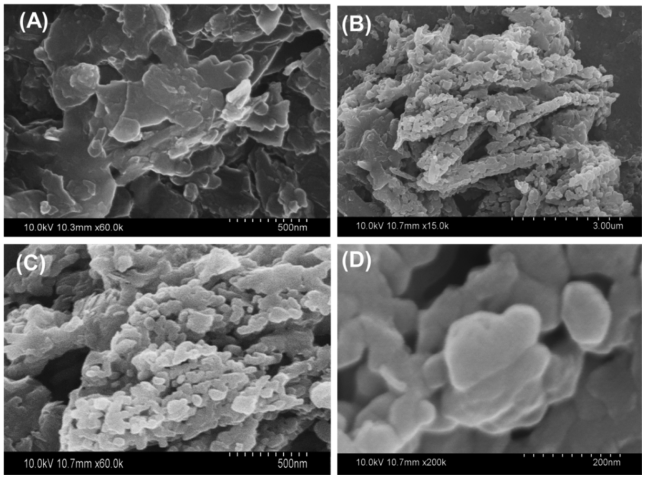

Figure 4. SEM images of raw clinoptilolite (A) and synthetic G.Na$^+$/Clino (B−D).

This was reflected in the determined surface area as the value increased from 258 m^2/g for the precursor sample up to 312 m^2/g for G.Na$^+$/Clino. This also appeared in the pore volume and pore diameter of both raw zeolite (18.2 nm pore diameter and 0.041 mL/g pore volume) and G.Na$^+$/Clino (17.2 nm pore diameter and 0.038 mL/g pore volume). The decline in the values is related to the formed secondary sodium silicate phase which might cause partial filling for some of the structural zeolite pores. Regarding the ion-exchange capacity, it increased from 132 mequiv/100 g for Clino up to 387 mequiv/100 g for G.Na$^+$/Clino. These two parameters (surface area and ion-exchange capacity) are essential factors in controlling the loading capacity and release properties of the studied carriers.

2.2. Loading Properties of G.Na$^+$/Clino for 5-Fu. *2.2.1. Effect of Loading Factors. 2.2.1.1. Effect of the Loading pH.* The solution pH during the loading process has a strong influence on the loading capacity of G.Na$^+$/Clino as a carrier. The solution pH directs the ionization behavior of the drug molecules as well as the charges of the solid carrier. The experimental effect of the solution pH on the loading performance of G.Na$^+$/Clino as a carrier for the 5-Fu drug was studied from pH 3 up to pH 10 (Figure 5A). The other affecting variables were fixed at 200 mg/L, 4 h, 20 mg, and 25 °C for the 5-Fu concentration, the loading period, the carrier quantity, and the loading temperature, respectively. Experimentally, the increase in the loading pH resulted in remarkable enhancement in the measured G.Na$^+$/Clino loading capacity. This was detected within the range from pH 3 (acidic conditions) to pH 9 (basic conditions) [54.3 mg/g (Clino) and 80.9 mg/g (G.Na$^+$/Clino)] (Figure 5A). The alkaline environments enhanced the ionization efficiency of the 5-Fu molecules to be of considerable stability and higher ionic interaction with the active loading sites of the G.Na$^+$/Clino carrier.[3,16] The observable decrease in the actual loading properties for the conducted tests at pH higher than 9 was assigned to the extensive existence of hydroxyl radicals over the surface of the inspected carrier (Figure 5A). Such negatively charged hydroxyl groups showed repulsive properties with the ions of the drug. Additionally, the high alkaline environment had a destructive and leaching effect on the structure of the G.Na$^+$/Clino carrier as an aluminosilicate material.[7,35] The previous behavior is of agreement with the measured pH$_{(PZC)}$

https://doi.org/10.1021/acsomega.1c06671
ACS Omega 2022, 7, 6991−7001

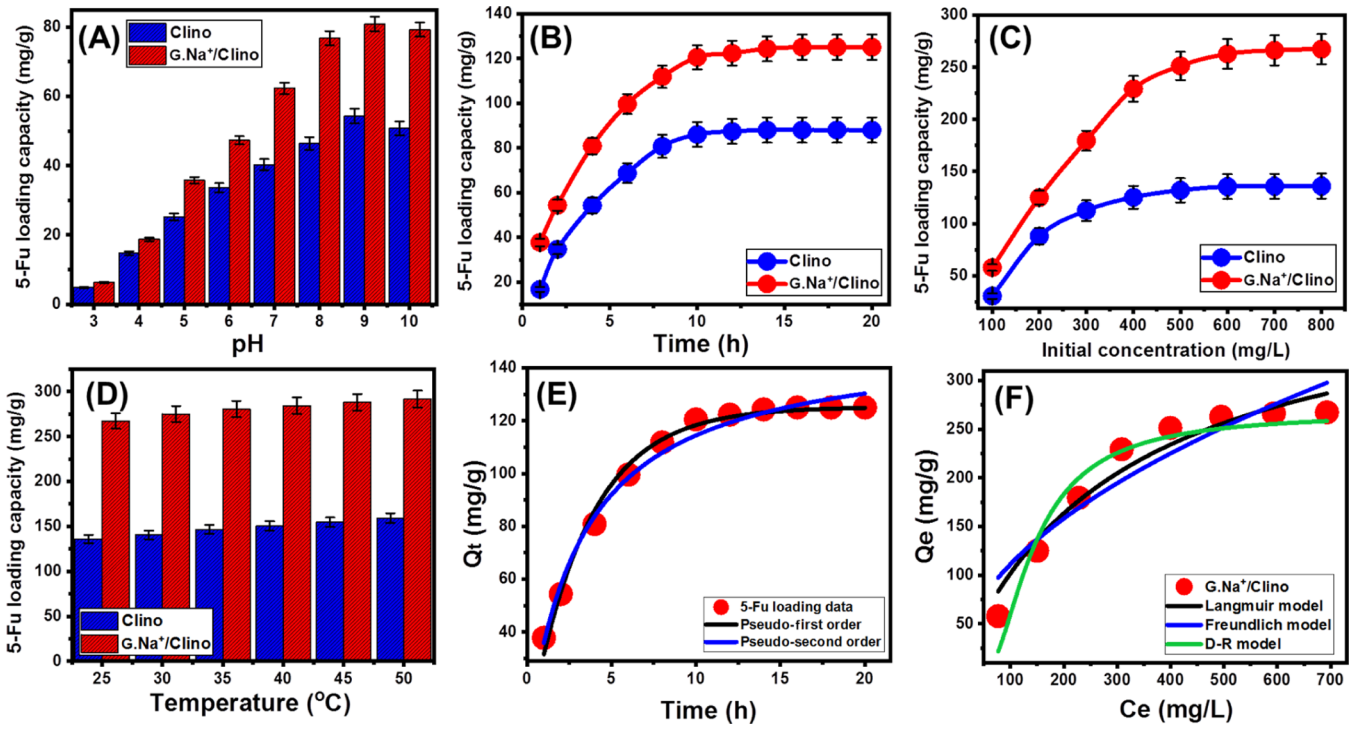

Figure 5. Effect of pH on the loading of 5-Fu into clino and G.Na$^+$/Clino (A), effect of time interval on the loading of 5-Fu into clino and G.Na$^+$/Clino (B), effect of the drug concentrations on the loading of 5-Fu into clino and G.Na$^+$/Clino (C), effect of temperature on the loading of 5-Fu into clino and G.Na$^+$/Clino (D), fitting of the 5-Fu loading results with the common kinetic models (E), and fitting of the 5-Fu loading results with the main isotherm models (F). Qt: Adsorption capacity at a certain time interval. Qe: Equilibrium adsorption capacity. Ce: Equilibrium concentration of As (V).

value of the G.Na$^+$/Clino carrier that is equal to 6.6, reflecting the saturation of its surface with negative charges at all the pH values which are higher than pH 6.6.

2.2.1.2. Effect of the Loading Interval. The effect of the loading interval was addressed within an experimental range from 1 h up to 20 h to detect the equilibration interval and the required time for the best loading capacity (Figure 5B). The other affecting variables were fixed at 200 mg/L, pH 9, 20 mg, and 25 °C for the 5-Fu concentration, the loading pH, the carrier quantity, and the loading temperature, respectively. The regular expansion in the loading period resulted in observable enhancement in the quantities of the loaded 5-Fu either by Clino or by G.Na$^+$/Clino (Figure 5B). This can be detected up to 12 h for Clino (88 mg/g) and 14 h for G.Na$^+$/Clino (125 mg/g). After that, the determining loading quantities showed very slight variation or nearly fixed, demonstrating the equilibration states of the carriers (Figure 5B). The presence of numerous free and active loading sites during the initial stages of the loading process resulted in the detected increment in the quantities of the adsorbed 5-Fu molecules. The consumption of such sites with time resulted in a decline in the loading quantities until the consumption or occupation of all the sites which minimized the chance for further loading and achieving the equilibration stage.[1]

2.2.1.3. Effect of the 5-Fu Concentration. Conducting the loading tests in the presence of different concentrations (100–800 mg/L) of 5-Fu molecules is of vital significance for the maximum loading capacity of the solid carriers (Figure 5C). The other affecting variables were fixed at 24 h, pH 9, 20 mg, and 25 °C for the loading period, the loading pH, the carrier quantity, and the loading temperature, respectively. The 5-Fu loading quantities by both Clino and G.Na$^+$/Clino increased strongly by performing the loading tests at high concentrations of the drug molecules up to 600 mg/L [Clino (136 mg/g) and G.Na$^+$/Clino (267.4 mg/g)] (Figure 5C). These capacities are the maximum 5-Fu quantities that can be loaded into the carriers, reflecting the complete occupation of all the active sites of Clino and G.Na$^+$/Clino. Increasing the loading quantities with testing of high 5-Fu concentrations is related to the predicted increase in the driving forces of 5-Fu as dissolved molecules that induce their interactions with present active loading sites.[27]

2.2.1.4. Effect of the Loading Temperature. The influence of the loading temperature was tested from 25 up to 60 °C with the other affecting variables set to 24 h, pH 9, 20 mg, and 800 mg/L for the loading period, the loading pH, the carrier quantity, and the drug concentration, respectively (Figure 5D). The high-temperature conditions resulted in the highest 5-Fu loading quantities either by Clino or by G.Na$^+$/Clino, declaring the endothermic properties of their loading system (Figure 5D). The recognized loading capacities at 60 °C are 159.2 and 291.7 mg/g for Clino and G.Na$^+$/Clino, respectively (Figure 5D).

The general finding of the loading studies demonstrates the technical value of the green Na$^+$ functionalization processes in enhancing the loading properties of natural clinoptilolite zeolite in a controlled manner. This is related to the impact of the functionalization process in enhancing the surface area, the ion-exchange capacity, and the exposure of the active −OH-bearing groups. Additionally, the formation of new reactive phases of sodium silicate structures and the capping of bio-phenols are of strong impact in enhancing the affinity of the resulting G.Na$^+$/Clino for the dissolved 5-Fu molecules.

https://doi.org/10.1021/acsomega.1c06671
ACS Omega 2022, 7, 6991−7001

2.2.2. Loading Mechanism. 2.2.2.1. Kinetic Studies. The pseudo-first-order as well as pseudo-second-order models were evaluated to describe the kinetic properties of the occurred 5-Fu loading reactions by the G.Na$^+$/Clino inorganic carrier. This was completed considering the non-linear fitting results with the representative equations of the models (Table S1). The fitting degrees were evaluated based on both the determination coefficient (R^2) and the Chi-squared (χ^2) test (Figure 5E; Table 1). The occurred 5-Fu loading reaction

Table 1. Theoretical Parameters of the Studied Kinetic Models, Equilibrium Models, Van't Hoff Formula, and Release Kinetic Models

model	parameters	
pseudo-first-order	K_1 (min^{-1})	0.290
	$qe_{(Cal)}$ (mg/g)	125.2
	R^2	0.98
	X^2	0.175
pseudo-second-order	K_2 (g mg^{-1} min^{-1})	0.002
	$qe_{(Cal)}$ (mg/g)	151.2
	R^2	0.99
	X^2	0.145
	Isotherm Models	
Langmuir	$q$max (mg/g)	462.7
	b (L/mg)	0.0025
	R^2	0.95
	X^2	2.28
	R_L	0.33−0.80
Freundlich	$1/n$	0.609
	k_F (mg/g)	5.73
	R^2	0.90
	X^2	5.13
D−R model	β (mol^2/kJ^2)	0.0059
	qm (mg/g)	257.3
	R^2	0.93
	X^2	3.65
	E (kJ/mol)	10.47
	Thermodynamics	
ΔG° (kJ mol^{-1})	298.15	−14.20
	303.15	−14.53
	308.15	−14.82
	313.15	−15.10
	318.15	−15.39
	323.15	−15.67
ΔH° (kJ mol^{-1})		3.14
ΔS° (J K^{-1} mol^{-1})		58.19

release kinetics		
	determination coefficient	
models	pH 1.2	pH 7.4
zero-order model	0.76	0.70
first-order model	0.96	0.97
Higuchi model	0.90	0.87
Hixson−Crowell model	0.55	0.57
Korsmeyer−Peppas model	0.89	0.90

using G.Na$^+$/Clino as an inorganic carrier follows the kinetic behavior of the pseudo-second-order model with slight preferences as compared to the kinetic assumption of the pseudo-first-order model. The suggested complex loading mechanisms involved chemical (electron-sharing, surface complexation, hydrogen bonding, ion-exchange process, and internal diffusion) and physical processes (electrostatic attraction) with dominant effects for the chemical processes.[4,36]

2.2.2.2. Equilibrium Studies. The equilibrium properties of 5-Fu loading reactions by G.Na$^+$/Clino involving the loading form, nature of loading reactions, and theoretical maximum loading capacity were studied based on the assumptions of Langmuir, Freundlich, and Dubinin−Radushkevich models (Table S1). Considering the non-linear fitting parameters (R^2 and χ^2), the occurred 5-Fu loading processes follow the Langmuir equilibrium properties. This involved the orientation of 5-Fu as loaded molecules in the monolayer form and loading of them by active centers distributed homogeneously on the surface of G.Na$^+$/Clino as the inorganic carrier[26] (Figure 5F and Table 1). Additionally, the calculated values of RL parameters at different 5-Fu concentrations declared the favorable properties of the loading reactions with a theoretical maximum loading capacity of 462.7 mg/g.

Considering the fitting parameters of the loading results with the D−R model, the Gaussian energy is 10.47 kJ/mol. This value is within the recognized range for the chemical processes and ion-exchange mechanisms but still very close to the suggested limits for the physical processes (Table 1).[27] Such equilibrium findings are in agreement with the kinetic findings and support the suggestion about the dominant effect of the chemical mechanisms during the loading processes.

2.2.2.3. Thermodynamic Studies. The thermodynamic properties were assessed considering the essential parameters of Gibbs free energies ($\Delta G°$), entropies ($\Delta S°$), and enthalpies ($\Delta H°$) within the temperature range from 25 to 60 °C. The obtained $\Delta G°$ values were calculated from eq 1, while both $\Delta S°$ and $\Delta H°$ were determined as theoretical fitting parameters for the linear regression fitting process with the van't Hoff equation (eq 2) (Figure 6).[1]

$$\Delta G° = -RT \ln K_c \tag{1}$$

$$\ln(K_c) = \frac{\Delta S°}{R} - \frac{\Delta H°}{RT} \tag{2}$$

The $\Delta G°$ values for the occurred 5-Fu loading reactions using G.Na$^+$/Clino have negatively signed values (Table 1). This declared the favorable and spontaneous nature of the occurred reactions at all the tested temperature values[37] (Table 1). For the $\Delta H°$ value, it was estimated as a positive value that characterizes the endothermic loading reactions. Also, the

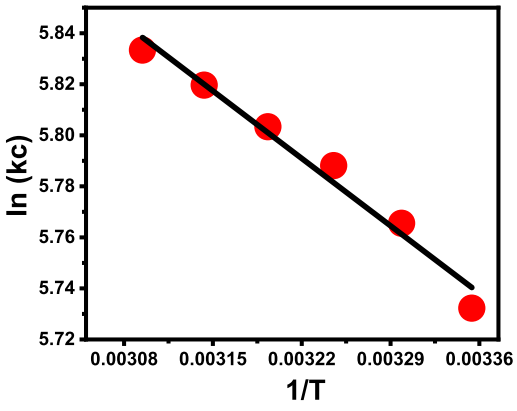

Figure 6. Fitting of the 5-Fu loading results with the van't Hoff equation.

https://doi.org/10.1021/acsomega.1c06671
ACS Omega 2022, 7, 6991−7001

positively determined value of entropy (ΔS°) suggested a remarkable enhancement in the randomness properties of the occurred 5-Fu loading reactions using G.Na^{+}/Clino (Table 1).

2.3. In Vitro Release Profiles. The actual release profile of G.Na^{+}/Clino as an inorganic carrier for the 5-Fu drug was assessed in a comparison study with pure clinoptilolite. This was evaluated considering the two releasing buffers [gastric fluid (pH 1.2) as well as intestinal fluid (pH 7.4)] (Figure 7A,B). Based on the release curves, the release processes

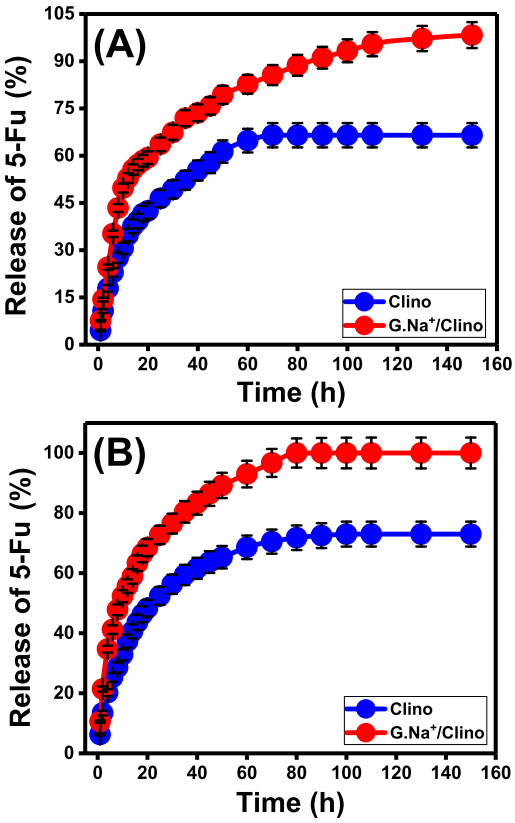

Figure 7. 5-Fu release profiles of Clino and G.Na^{+}/Clino in the gastric fluid (pH 1.2) (A) and intestinal fluid (pH 7.4) (B).

exhibit segmental curves of two distinguished segments that reflect the release of the drug according to two different rates either at pH 7.4 or at pH 1.2 (Figure 7A,B). The first segment declared the abrupt diffusion for the loaded 5-Fu molecules from both clinoptilolite and G.Na^{+}/Clino carrier. This might be related to the desorption of 5-Fu molecules by the surficial active sites of the carriers.[4,8] The second release segment had a faint diffusion rate for the loaded 5-Fu molecules. The release process at this stage is restricted only to the entrapped 5-Fu molecules within the structural channels of zeolite and the strongly binding molecules with functional groups of the carriers which reduce the diffusion efficiency.[3,38]

The recognized profile for clinoptilolite before the modification processes shows a slow and long release behavior up to 150 h achieving the complete release state in either the acidic fluid (pH 1.2) or the basic fluid (pH 7.4) (Figure 7A,B). The observed release percentages of 66.4% (70 h) and 73% (100 h) were detected as the actual maximum release values in the acidic fluid and the basic fluid, respectively (Figure 7A,B). The observed slow diffusion rate for 5-Fu as a loaded drug might be related to (A) the expected trapping of 5-Fu molecules within the structural channels of zeolite and (B) the bonding between the chemical groups of the drug and siloxane chemical groups of zeolite.[26,38] The high diffusion rate of 5-Fu in the basic fluid (pH 7.4) is related to the enhancement in the ionization properties of 5-Fu drug in alkaline environments which induce the solubility and the diffusion properties.[10,39] This is not recommended in several studies as it might cause an increase in the required dosages to match the target therapeutic level.

The recognized profile for G.Na^{+}/Clino exhibits higher diffusion properties than untreated clinoptilolite considering the acidic fluid (pH 1.2) as well as the basic fluid (pH 7.4) (Figure 7A,B). 50% of the loaded 5-Fu dosage was released after 12 and 10 h in the acidic fluid (pH 1.2) and basic fluid (pH 7.4), respectively. Moreover, 95% of the 5-Fu dosage diffused from the G.Na^{+}/Clino carrier after 120 h (pH 1.2) and 70 h (pH 7.4) (Figure 7A,B). Considering the aforementioned results and behaviors, the synthetic G.Na^{+}/Clino composite is of significant technical qualifications to be applied as an inorganic carrier for the 5-Fu drug. The loaded dosage of the 5-Fu drug can be delivered to the human system according to the recommended therapeutic level by controlling the functionalization process and the quantities of the green sodium ions. The recognized acceleration in the 5-Fu diffusion rate from the structure of G.Na^{+}/Clino as compared to the untreated clinoptilolite might be attributed to the increase in the ion-exchange capacity and the partial filling of the zeolite pores by the formed sodium silicate phase.

2.4. Release Kinetics. The release kinetic modeling was applied to follow the expected mechanisms which might control the release reactions from the structure of G.Na^{+}/Clino as an inorganic drug carrier. This was performed considering the linear regression fitting degrees of the release results with zero-order (eq 3), first-order (eq 4), Higuchi (eq 5), Hixson–Crowell (eq 6), and Korsmeyer–Peppas (eq 7) release kinetic models.[4]

$$W_t - W_0 = K_0 \cdot t \tag{3}$$

$$\ln(W_\infty / W_t) = K_1 \cdot t \tag{4}$$

$$W_t = K_h t^{1/2} \tag{5}$$

$$W_0^{1/3} - W_t^{1/3} = K_{HC} t \tag{6}$$

$$W_t / W_\infty = K_p t^n \tag{7}$$

The diffusion of 5-Fu according to the zero-order assumption involves a release process of the constant rate and is independent of the loaded 5-Fu dosages.[40] The reverse can be reported for the release processes that are of first-order kinetic behavior.[1,41] The release reactions that are of Higuchi kinetics are controlled by the molecule diffusion mechanisms considering six associated processes. The associated processes involved the following: (A) the diffused molecules are lower than the loaded dosages, (B) the diffusion of the molecules is restricted to only one direction, (C) synthesis of a carrier with a thickness higher than the diameter of the investigated drug, (D) the diffusion rates are independent of both the swelling and solubility properties of the solid carrier, the diffusion process occurs according to the constant rate during the entire release period, and (F) the test drug should be of sink properties.[1,4,41] The release reactions that follow Hixson–Crowell kinetics involve the erosion processes as the main

https://doi.org/10.1021/acsomega.1c06671
ACS Omega 2022, 7, 6991−7001

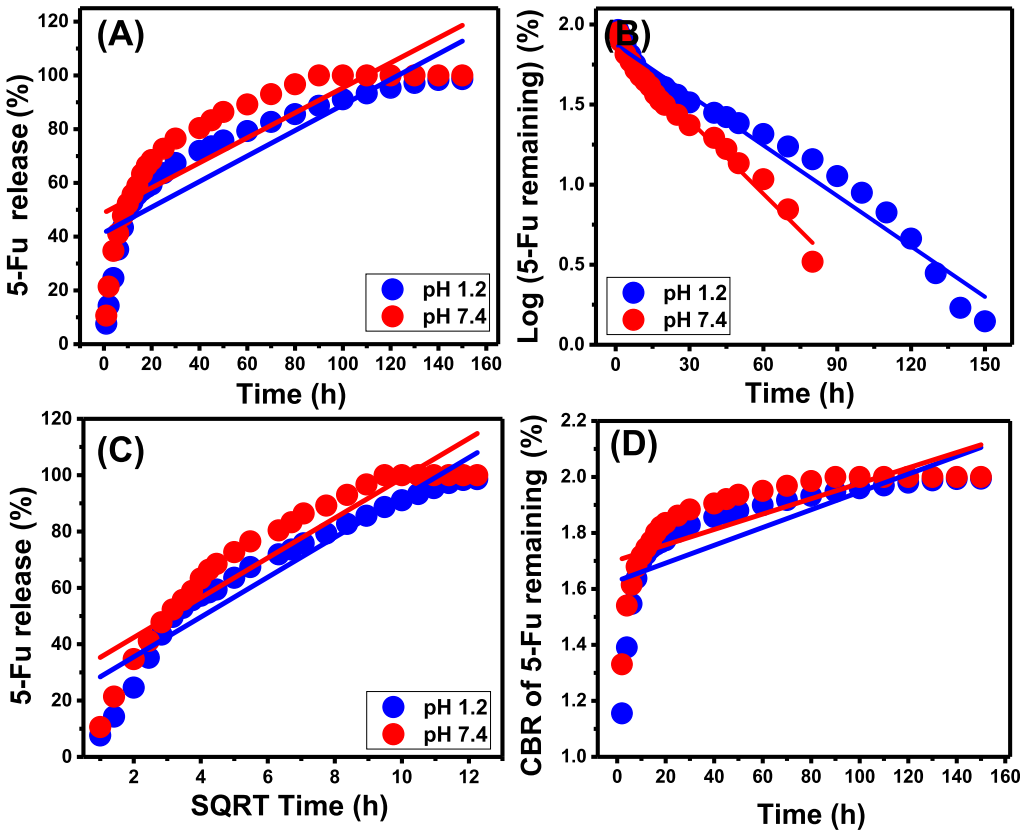

Figure 8. Fitting of the recognized 5-Fu release results with the zero-order model (A), first-order model (B), Higuchi model (C), and Hixson–Crowell model (D).

release mechanism. Moreover, the release process depends strongly on the diameter of the solid particles as well as the surface area.[42] The occurrence of the release reactions according to the Korsmeyer–Peppas kinetics demonstrates the presence of both diffusion and erosion processes as the release mechanisms.[26]

Based on the obtained fitting degrees for the linear regression fitting processes, the 5-Fu release reactions follow the first-order kinetic model (Figure 8B; Table 1) rather than the zero-order model (Figure 8B; Table 1). This signifies the remarkable influence of the loaded 5-Fu dosages on the efficiency of the release processes at both pH 1.2 (acidic fluid) and pH 7.4 (basic fluid). Additionally, the fitting processes of the release results show an observable agreement with Higuchi kinetics (Figure 8C; Table 1) as compared to Hixson–Crowell (Figure 8D; Table 1) kinetics. This suggested an essential effect for the erosion mechanisms during the occurred 5-Fu release reactions with a dominant role for the diffusion processes. The diffusion mechanism might be related to the desorption of the 5-Fu molecules which were loaded into the surficial or exchangeable sites of G.Na^+/Clino as an inorganic drug carrier. The previous findings were supported by the reported high fitting of the 5-Fu release results with the assumption of Korsmeyer–Peppas kinetics (Figure 9; Table 1). The values of the model diffusion exponent (n) are 0.42 and 0.37 for the release processes at pH 1.2 and pH 7.4, respectively. These values are within the recognized range for the non-Fickian transport process for the loaded drug, involving erosion as well as diffusion as controlling mechanisms. Considering the other studied release kinetic models, the release process occurred essentially by the

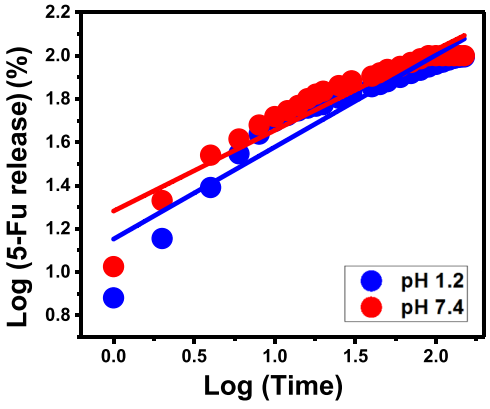

Figure 9. Fitting of the recognized 5-Fu release results with the Korsmeyer–Peppas model.

diffusion mechanism in addition to the assistant role of the erosion mechanisms. The erosion processes can be detected strongly in the basic fluid (pH 7.4) and related to the partial dissolution of the clinoptilolite structure, as aluminosilicate materials under such conditions and acidic conditions might be related to the predicted leaching of Al ions.

2.5. Comparison Study. The loading, as well as the release properties, of G.Na^+/Clino as an inorganic carrier for the 5-Fu drug were compared with other studied carriers in literature. The recognized 5-Fu loading capacity of G.Na^+/Clino is higher than several investigated carriers (Table 2). Such high technical and commercial value of the product enables the composite to be applied as a delivery system for the 5-Fu drug. This is of valuable impact in reducing the quantities

https://doi.org/10.1021/acsomega.1c06671
ACS Omega 2022, 7, 6991−7001

Table 2. Comparison between the Loading Capacities and Release Periods of the Studied Carrier and Other Carriers in Literature

carrier	loading capacity (mg/g)	release period	references
montmorillonite/magnetite	59.44	24 h	7
magadiite	98.18		43
chitosan/MCM-48	191	80 h	3
Ca-montmorillonite	23.3		44
magadiite−CTAB−chitosan	162.29		43
HY zeolite	110	5 h	45
magadiite−CTAB	130.59		43
montmorillonite	90		46
clinoptilolite	138.9	150 h	this study
G.Na^+/Clino	462	150	this study

of the used solid carriers as well as the concentrations of 5-Fu as discharged pharmaceutical residuals. Additionally, the synthetic G.Na^+/Clino carrier has a continuous and considerably longer release profile (150 h) than the presented carriers. Therefore, the synthetic G.Na^+/Clino as an inorganic has valuable technical properties to deliver the loaded 5-Fu drug at controlled rates and specific dosages based on the recommended therapeutic values.

2.6. Cytotoxicity Results. The cytotoxicity properties were evaluated based on the cell viability percentages according to the MTT assay method. Regarding the normal colorectal fibroblast cells (CCD-18Co), the synthetic G.Na^+/Clino carrier has remarkable biocompatibility, safety, and a weak cytotoxic impact on the normal cells for all the investigated dosages (0−300 μg/mL). The determined cell viability percentage using the highest dosage of G.Na^+/Clino (300 μg/mL) is 85.4% (Figure 10A).

For the investigated colon cancer cells (HCT-116), the cell viability values using 5-Fu-loaded G.Na^+/Clino were determined in comparison with those of free 5-Fu molecules. The measured cell viability percentages show a recognizable decline with testing of free 5-Fu and 5-Fu-loaded G.Na^+/Clino at high dosages or concentrations up to 300 μg/mL (Figure 10B). The obtained cell viability percentages using 5-Fu-loaded G.Na^+/Clino are lower than the measured values using the values of free 5-Fu drug considering all the incorporated concentrations (Figure 10B). The measured cell viability percentages in the presence of the highest free 5-Fu and 5-Fu-loaded G.Na^+/Clino concentration (300 μg/mL) are 34 and 7.3%, respectively. Such findings declared a remarkable impact for the used G.Na^+/Clino carrier in inducing the cytotoxic effect of the 5-Fu drug on colon cancer cells. This might be attributed to the homogeneous distribution of the 5-Fu drug over the structure of the synthetic G.Na^+/Clino carrier which increases the exposure of the drug molecules as well as the interaction area. Additionally, the diffusion of 5-Fu molecules by regular rates has an enhanced impact on the target HCT-116 cells. Therefore, the synthetic G.Na^+/Clino as an inorganic carrier for the 5-Fu drug has valuable biocompatible and safe properties in addition to its role in inducing the solubility and the cytotoxicity of the loaded drug.

3. CONCLUSIONS

Na^+ green-functionalized clinoptilolite (G.Na^+/Clino) was synthesized as an enhanced inorganic carrier (312 m^2/g surface area and 387 mequiv/100 g ion-exchange capacity) for the commonly used chemotherapy 5-Fu drug. The recognized 5-Fu loading capacity of G.Na^+/Clino was 462 mg/g, which is an enhanced value considering the untreated zeolite and the other studied inorganic carriers. The kinetic assumptions of the pseudo-second-order model and equilibrium significances of the Langmuir model were used to describe the 5-Fu loading into G.Na^+/Clino. The equilibrium findings in addition to the Gaussian energy (10.47 kJ/mol) and the thermodynamic parameters declared the homogeneous, more chemical, endothermic, and spontaneous properties of the 5-Fu loading reactions. The assessed release profile of G.Na^+/Clino as a carrier for 5-Fu is regular and showed slow rate properties up to 150 h at pH 1.2 and 80 h at pH 7.4. The release kinetic investigation suggested complex diffusion/erosion release mechanisms for 5-Fu from the G.Na^+/Clino carrier. The cytotoxicity of G.Na^+/Clino and 5-Fu-loaded G.Na^+/Clino demonstrated a remarkable safe effect of the carrier on the fresh cells (CCD-18Co) and a significant enhancement effect for the impact of the loaded drug on the cancer cells (HCT-116).

4. EXPERIMENTAL WORK

4.1. Materials. Samples of natural clinoptilolite mineral composed of SiO_2 (68.39%), Al_2O_3 (11.52%), K_2O (4.06%), Fe_2O_3 (2.676%), MgO (0.483%), Na_2O (0.38%), CaO (1.65%), and L.O.I (10.99%) with the major oxide content

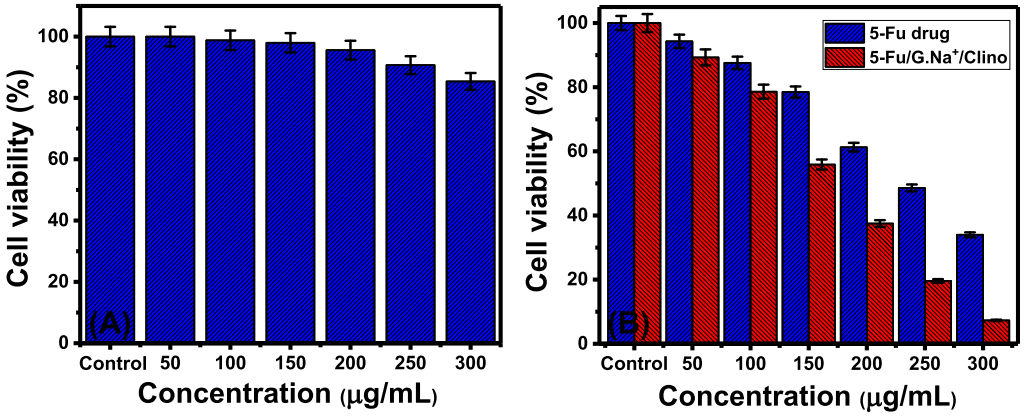

Figure 10. In vitro cytotoxicity properties of G.Na^+/Clino on the normal colorectal fibroblast cell (CCD-18Co) (A) and of free 5-Fu drug and 5-Fu-loaded G.Na^+/Clino on colon cancer cells (HCT-116) (B).

https://doi.org/10.1021/acsomega.1c06671
ACS Omega 2022, 7, 6991−7001

were obtained. Sodium nitrite (>97%, Aldrich) and green tea leaves were used for the green modification process of clinoptilolite with Na^+ ions. The extract of the used leaves was applied as both reducing and stabilizing agents based on its components of phenols and caffeine. The 5-Fu drug (analytical grade, > 99% purity) was obtained from Sigma-Aldrich Company and was assessed in systematic loading and release studies.

4.2. Na^+ Green Functionalization of Clinoptilolite (G.Na^+/Clino). Prior to the clinoptilolite modification process, the samples were ground using a ball mill for 8 h as the initial mechanical activation step. After that, 3 g of ground fractions was dispersed in 50 mL of deionized water containing 2.5 g of sodium nitrite ($NaNO_2$). This was followed by stirring for 90 min at 500 rpm in the presence of a sonication source with power (240 W) at an optimized pH of 8 and at room temperature of 25 °C. Then, the green tea extract (50 mL) that was prepared by direct boiling of the tea leaves for 5 min was added at once to the clinoptilolite/$NaNO_2$ mixture under vigorous stirring for 2 h. This was followed by an additional sonication treatment for 2 h at the same temperature and pH. The system was then left at ambient temperature overnight to ensure the effective interaction between the incorporated reactants. The obtained solid product was then separated from the extract solution, washed several times with distilled water, and finally dried at 70 °C for 12 h. The modified product was labeled as G.Na^+/Clino and kept for further characterization and application.

4.3. Characterization of the G.Na^+/Clino Carrier. Different crystalline phases and their structural properties were investigated using a PANalytical X-ray diffraction instrument (Empyrean) from 5 to 70° under the adjusted voltage at 40 kV. The morphological features were observed using a scanning electron microscope (Gemini, Zeiss-Ultra 55) at 30 kV accelerating voltage. The structural chemical groups and the elemental composition were figured out using FT-IR spectroscopy (FT-IR-8400S) and energy-dispersive X-ray spectrometry (EDX), respectively. The frequency range of FT-IR detection was from 400 to 400 cm^{-1} with the scan degree and resolution set to 37° and 4 cm^{-1}, respectively. A surface area analyzer device (Beckman Coulter; SA3100) was used to study the surface area as well as the porosity properties in the degassing process at 77 K. The obtained ion-exchange capacities were measured based on the $BaCl_2$ method. A Zetasizer attached with a zeta cell (Malvern, version 7.11) was employed to determine the zeta potential values at different pHs during the estimation of pH at zero point charge ($pH_{(ZPC)}$).

4.4. Loading of the 5-Fu Drug. The loading behavior was assessed based on the common experimental factors including the 5-Fu concentration (100−800 mg/L), pH (3−10), loading intervals (1−20 h), and temperature (25−50 °C). The mixing between the fractions of the carrier and the drug solutions was performed using a vortex rotator instrument. After the inspected equilibration period, the solid fractions were separated from the drug solutions by the centrifugation process. The residual 5-Fu concentrations in the samples were determined using a UV-spectrophotometer device at a λ (max) value of 266 nm. The experiments were carried out in triplicate form considering the average results during the evaluation steps with a standard deviation of less than 3.8%. The 5-Fu loading capacity of G.Na^+/Clino in milligram per gram was calculated according to eq 8.[40]

$$\text{loaded drug capacity (mg/g)} = [(\text{initial concentration} - \text{remaining concentration}) \times \text{solvent volume}]/[\text{weight of carrier}] \quad (8)$$

4.5. In Vitro Release Profile. The release properties of 5-Fu from the G.Na^+/Clino carrier were inspected at pH 1.2 (gastric fluid) and pH 7.4 (intestinal fluid), and the temperature was adjusted to 37.5 °C. A specific amount of G.Na^+/Clino loaded with 100 mg/g of 5-Fu was dispersed within fixed volumes of the two buffers (500 mL) for a total release interval of 150 h. The homogenization between the fractions of the carrier and the buffers was achieved using a dissolution instrument (Distek type, 4300) at 200 rpm rotating speed. At regular periods, 5 mL of the release buffers was separated to determine the concentrations of the released 5-Fu by a UV-spectrophotometer device at a λ (max) value of 266 nm. After that, the separated volume was added again to the bulk solutions of the buffers. The release tests were also carried out in triplicate, and the results were obtained as their average values considering the standard deviation (less than 4.23%). The release percentages of 5-Fu from G.Na^+/Clino were calculated according to eq 9.[1]

$$\text{Drug release}(\%) = \frac{\text{the amount of released 5-Fu drug}}{\text{amount of loaded 5-Fu}} \times 100 \quad (9)$$

4.6. In Vitro Cytotoxicity Studies. *4.6.1. Cell Lines and Used Reagents.* The normal colorectal fibroblast human cell line (CCD-18Co) and the colon cancer cell line (HCT-116) (CCAT, Rockville, MD) were used to evaluate the cytotoxicity properties of G.Na^+/Clino and 5-Fu-loaded G.Na^+/Clino. HEPES buffer solution, RPMI-1640, dimethyl sulfoxide (DMSO, 99%), gentamycin, 3(4,5-dimethylthiazol-2-yl)-2.5 diphenyltetrazolium bromide (MTT, 99%), fetal bovine serum, 0.25% trypsin−ethylenediaminetetraacetic acid, and Dulbecco's modified Eagles medium (St. Louis, Mo., USA) were the reagents used during the tests. All the tests were conducted at the Regional Center for Mycology& Biotechnology, Al-Azhar University, Egypt.

4.6.2. In Vitro Cytotoxicity. The CCD-18Co and HCT-116 cell lines were incubated in RPMI-1640 growth medium which was supplemented with gentamycin (50 μg/mL) and fetal calf serum (10%) at 37 °C in a humidified atmosphere (5% CO_2). The culture process was repeated three times regularly per week. After that, the studied cell lines were incorporated into Corning-96-well plates at the concentration of 5×10^4 cells/well and incubated for 24 h. After this step, the G.Na^+/Clino- and 5-Fu-loaded G.Na^+/Clino fractions were added at regular dosages (0 μg/mL up to 300 μg/mL) and incubated for additional 24 h. The resultant viable cells were then determined by the MTT assay method based on the measured results for the incorporated control samples.

Upon completion of the exposure interval, the incorporated culture medium was removed effectively and replaced by a new and fresh medium (100 μL of RPMI). Prior to the second incubation step (5 h), MTT (10 μL; 12 mM) was added carefully to the inspected cell wells in the same growth environment. After a certain interval, the resulting formazan was removed from the system by dissolving it using DMS (50 μL). As a final step, the optical densities were used as indicators for the values of cell viability values based on eq 10.

https://doi.org/10.1021/acsomega.1c06671
ACS Omega 2022, 7, 6991−7001

The optical density was measured by a microplate reader considering the measuring wavelength at 590 nm.

$$\text{Cell viability (\%)} = \frac{\text{mean OD}}{\text{control OD}} \times 100 \quad (10)$$

■ ASSOCIATED CONTENT

Supporting Information

The Supporting Information is available free of charge at https://pubs.acs.org/doi/10.1021/acsomega.1c06671.

Representative equations of the kinetic and isotherm models (PDF)

■ AUTHOR INFORMATION

Corresponding Author

Mostafa R. Abukhadra − *Materials Technologies and Their Applications Lab, Geology Department, Faculty of Science, Beni-Suef University, 62514 Beni Suef City, Egypt; Geology Department, Faculty of Science, Beni-Suef University, 62514 Beni-Suef, Egypt;* orcid.org/0000-0001-5404-7996; Email: Abukhadra89@Scinec.bsu.edu.eg

Authors

Mohamed Adel Sayed − *Materials Technologies and Their Applications Lab, Geology Department, Faculty of Science, Beni-Suef University, 62514 Beni Suef City, Egypt; Department of Chemistry, Faculty of Science, Beni-Suef University, 62514 Beni-Suef City, Egypt*

Hayam M. El-Zeiny − *Materials Technologies and Their Applications Lab, Geology Department, Faculty of Science, Beni-Suef University, 62514 Beni Suef City, Egypt; Department of Chemistry, Faculty of Science, Beni-Suef University, 62514 Beni-Suef City, Egypt*

Jong Seong Khim − *School of Earth & Environmental Sciences, College of Natural Sciences, Seoul National University, 08826 Seoul, Republic of Korea*

Jamaan S. Ajarem − *Zoology Department, College of Science, King Saud University, 12371 Riyadh, Saudi Arabia*

Ahmed A. Allam − *Zoology Department, Faculty of Science, Beni-Suef University, 62514 Beni-Suef, Egypt*

Complete contact information is available at: https://pubs.acs.org/10.1021/acsomega.1c06671

Author Contributions

This article was written through the contributions of all authors. All authors have given approval to the final version of the manuscript.

Notes

The authors declare no competing financial interest.

Further economic and commercial studies will be conducted to investigate the predict cost of the synthetic products as drug delivery system in the industrial scale.

■ ACKNOWLEDGMENTS

The authors acknowledge Researchers Supporting Project no (RSP-2021/149), King Saud University, Riyadh, Saudi Arabia.

■ REFERENCES

(1) El-Zeiny, H. M.; Abukhadra, M. R.; Sayed, O. M.; Osman, A. H. M.; Ahmed, S. A. Insight into novel β-cyclodextrin-grafted-poly (N-vinylcaprolactam) nanogel structures as advanced carriers for 5-fluorouracil: Equilibrium behavior and pharmacokinetic modeling. *Colloids Surf., A* **2020**, *586*, 124197.

(2) Cutrim, E. S. M.; Vale, A. A. M.; Manzani, D.; Barud, H. S.; Rodríguez-Castellón, E.; Santos, A. P. S. A.; Alcântara, A. C. S. Preparation, characterization and in vitro anticancer performance of nanoconjugate based on carbon quantum dots and 5-Fluorouracil. *Mater. Sci. Eng., C* **2021**, *120*, 111781.

(3) Abukhadra, M. R.; Refay, N. M.; El-Sherbeeny, A. M.; El-Meligy, M. A. Insight into the Loading and Release Properties of MCM-48/Biopolymer Composites as Carriers for 5-Fluorouracil: Equilibrium Modeling and Pharmacokinetic Studies. *ACS Omega* **2020**, *5*, 11745−11755.

(4) Othman, S. I.; Allam, A. A.; Al Fassam, H.; Abu-Taweel, G. M.; Altoom, N.; Abukhadra, M. R. Sonoco Green Decoration of Clinoptilolite with MgO Nanoparticles as a Potential Carrier for 5-Fluorouracil Drug: Loading Behavior, Release Profile, and Cytotoxicity. *J. Inorg. Organomet. Polym. Mater.* **2021**, *31*, 4608−4622.

(5) Mallikarjuna Reddy, K.; Ramesh Babu, V.; Krishna Rao, K. S. V.; Subha, M. C. S.; Chowdoji Rao, K.; Sairam, M.; Aminabhavi, T. M. Temperature sensitive semi-IPN microspheres from sodium alginate and N-isopropylacrylamide for controlled release of 5-fluorouracil. *J. Appl. Polym. Sci.* **2008**, *107*, 2820−2829.

(6) Rudzinski, W. E.; Palacios, A.; Ahmed, A.; Lane, M. A.; Aminabhavi, T. M. Targeted delivery of small interfering RNA to colon cancer cells using chitosan and PEGylated chitosan nanoparticles. *Carbohydr. Polym.* **2016**, *147*, 323−332.

(7) Chaturvedi, K.; Kulkarni, A. R.; Aminabhavi, T. M. Blend microspheres of poly (3-hydroxybutyrate) and cellulose acetate phthalate for colon delivery of 5-fluorouracil. *Ind. Eng. Chem. Res.* **2011**, *50*, 10414−10423.

(8) Tan, D.; Yuan, P.; Dong, F.; He, H.; Sun, S.; Liu, Z. Selective loading of 5-fluorouracil in the interlayer space of methoxy-modified kaolinite for controlled release. *Appl. Clay Sci.* **2018**, *159*, 102−106.

(9) Abukhadra, M. R.; Refay, N. M.; El-Sherbeeny, A. M.; Mostafa, A. M.; Elmeligy, M. A. Facile synthesis of bentonite/biopolymer composites as low-cost carriers for 5-fluorouracil drug; equilibrium studies and pharmacokinetic behavior. *Int. J. Biol. Macromol.* **2019**, *141*, 721−731.

(10) Vatanparast, M.; Shariatinia, Z. AlN and AlP doped graphene quantum dots as novel drug delivery systems for 5-fluorouracil drug: theoretical studies. *J. Fluorine Chem.* **2018**, *211*, 81−93.

(11) Macedo, L. D. O.; Barbosa, E. J.; Löbenberg, R.; Bou-Chacra, N. A. Anti-inflammatory drug nanocrystals: state of art and regulatory perspective. *Eur. J. Pharm. Sci.* **2021**, *158*, 105654.

(12) Lu, C.; Xiao, Y.; Liu, Y.; Sun, F.; Qiu, Y.; Mu, H.; Duan, J. Hyaluronic acid-based levofloxacin nanomicelles for nitric oxide-triggered drug delivery to treat bacterial infections. *Carbohydr. Polym.* **2020**, *229*, 115479.

(13) Khang, M. K.; Zhou, J.; Co, C. M.; Li, S.; Tang, L. A pretargeting nanoplatform for imaging and enhancing anti-inflammatory drug delivery. *Biomaterials* **2020**, *5*, 1102−1112.

(14) Sur, S.; Rathore, A.; Dave, V.; Reddy, K. R.; Chouhan, R. S.; Sadhu, V. Recent developments in functionalized polymer nanoparticles for efficient drug delivery system. *Nano-Struct. Nano-Objects* **2019**, *20*, 100397.

(15) Ganguly, K.; Kulkarni, A. R.; Aminabhavi, T. M. In vitro cytotoxicity and in vivo efficacy of 5-fluorouracil-loaded enteric-coated PEG-cross-linked chitosan microspheres in colorectal cancer therapy in rats. *Drug Deliv.* **2016**, *23*, 2838−2851.

(16) Spanakis, M.; Bouropoulos, N.; Theodoropoulos, D.; Sygellou, L.; Ewart, S.; Moschovi, A. M.; Siokou, A.; Niopas, I.; Kachrimanis, K.; Nikolakis, V.; Cox, P. A.; Vizirianakis, I. S.; Fatouros, D. G. Controlled release of 5-fluorouracil from microporous zeolites. *Nanomed. Nanotechnol. Biol. Med.* **2014**, *10*, 197−205.

(17) Jin, L.; Liu, Q.; Sun, Z.; Ni, X.; Wei, M. Preparation of 5-fluorouracil/β-cyclodextrin complex intercalated in layered double hydroxide and the controlled drug release properties. *Ind. Eng. Chem. Res.* **2010**, *49*, 11176−11181.

(18) Elboughdiri, N. The use of natural zeolite to remove heavy metals Cu (II), Pb (II) and Cd (II), from industrial wastewater. *Cogent Eng.* **2020**, *7*, 1782623.
(19) Vasylechko, V. O.; Klyuchivska, O. G. Y.; Manko, N. O.; Gryshchouk, G. V.; Kalychak, Y. M.; Zhmurko, I. I.; Stoika, R. S. Novel nanocomposite materials of silver-exchanged clinoptilolite with pre-concentration of Ag $(NH_3)^{2+}$ in water possess enhanced anticancer action. *Appl. Nanosci.* **2020**, *10*, 4869−4878.
(20) Servatan, M.; Zarrintaj, P.; Mahmodi, G.; Kim, S.-J.; Ganjali, M. R.; Saeb, M. R.; Mozafari, M. Zeolites in drug delivery: Progress, challenges and opportunities. *Drug Discov. Today* **2020**, *25*, 642−656.
(21) Sandomierski, M.; Buchwald, Z.; Koczorowski, W.; Voelkel, A. Calcium forms of zeolites A and X as fillers in dental restorative materials with remineralizing potential. *Microporous Mesoporous Mater.* **2020**, *294*, 109899.
(22) Yaneva, Z.; Ivanova, D.; Popov, N. Clinoptilolite Microparticles as Carriers of Catechin-Rich Acacia catechu Extracts: Micro-encapsulation and In Vitro Release Study. *Molecules* **2021**, *26*, 1655.
(23) Pavelić, S. K.; Medica, J.; Gumbarević, D.; Filošević, A.; Pržulj, N.; Pavelić, K. Critical review on zeolite clinoptilolite safety and medical applications in vivo. *Front. Pharmacol.* **2018**, *9*, 1350.
(24) Vargas, A. M.; Cipagauta-Ardila, C. C.; Molina-Velasco, D. R.; Ríos-Reyes, C. A. Surfactant-modified natural zeolites as carriers for diclofenac sodium release: A preliminary feasibility study for pharmaceutical applications. *Mater. Chem. Phys.* **2020**, *256*, 123644.
(25) Souza, I. M. S.; Sainz-Díaz, C. I.; Viseras, C.; Pergher, S. B. C. Adsorption capacity evaluation of zeolites as carrier of isoniazid. *Microporous Mesoporous Mater.* **2020**, *292*, 109733.
(26) Mostafa, M.; El-Meligy, M. A.; Sharaf, M.; Soliman, A. T.; AbuKhadra, M. R. Insight into chitosan/zeolite-A nanocomposite as an advanced carrier for levofloxacin and its anti-inflammatory properties; loading, release, and anti-inflammatory studies. *Int. J. Biol. Macromol.* **2021**, *179*, 206−216.
(27) Salam, M. A.; AbuKhadra, M. R.; Mohamed, A. S. Effective oxidation of methyl parathion pesticide in water over recycled glass based-MCM-41 decorated by green Co_3O_4 nanoparticles. *Environ. Pollut.* **2020**, *259*, 113874.
(28) Mohamed, A. S.; Abukkhadra, M. R.; Abdallah, E. A.; El-Sherbeeny, A. M.; Mahmoud, R. K. The photocatalytic performance of silica fume based Co_3O_4/MCM-41 green nanocomposite for instantaneous degradation of Omethoate pesticide under visible light. *J. Photochem. Photobiol., A* **2020**, *392*, 112434.
(29) Abukhadra, M. R.; Basyouny, M. G.; El-Sherbeeny, A. M.; El-Meligy, M. A.; Luqman, M. Insights into the green doping of clinoptilolite with Na^+ ions (Na^+/Clino) as a nanocatalyst in the conversion of palm oil into biodiesel; optimization and mechanism. *Nanotechnology* **2021**, *32*, 155702.
(30) Basyouny, M. G.; Abukhadra, M. R.; Alkhaledi, K.; El-Sherbeeny, A. M.; El-Meligy, M. A.; Soliman, A. T. A.; Luqman, M. Insight into the catalytic transformation of the waste products of some edible oils (corn oil and palm oil) into biodiesel using MgO/clinoptilolite green nanocomposite. *Mol. Catal.* **2021**, *500*, 111340.
(31) Shaban, M.; Abukhadra, M. R. Geochemical evaluation and environmental application of Yemeni natural zeolite as sorbent for Cd^{2+} from solution: kinetic modeling, equilibrium studies, and statistical optimization. *Environ. Earth Sci.* **2017**, *76*, 310.
(32) Shaban, M.; Sayed, M. I.; Shahien, M. G.; Abukhadra, M. R.; Ahmed, Z. M. Adsorption behavior of inorganic-and organic-modified kaolinite for Congo red dye from water, kinetic modeling, and equilibrium studies. *J. Sol. Gel Sci. Technol.* **2018**, *87*, 427−441.
(33) Safwat, M. A.; Soliman, G. M.; Sayed, D.; Attia, M. A. Gold nanoparticles enhance 5-fluorouracil anticancer efficacy against colorectal cancer cells. *Int. J. Pharm.* **2016**, *513*, 648−658.
(34) Luo, H.; Ji, D.; Li, C.; Zhu, Y.; Xiong, G.; Wan, Y. Layered nanohydroxyapatite as a novel nanocarrier for controlled delivery of 5-fluorouracil. *Int. J. Pharm.* **2016**, *513*, 17−25.
(35) Li, Z.; Zhang, B.; Jia, S.; Ma, M.; Hao, J. Novel supramolecular organogel based on β-cyclodextrin as a green drug carrier for enhancing anticancer effects. *J. Mol. Liq.* **2018**, *250*, 19−25.
(36) Liu, Y.; Yan, C.; Zhao, J.; Zhang, Z.; Wang, H.; Zhou, S.; Wu, L. Synthesis of zeolite P1 from fly ash under solvent-free conditions for ammonium removal from water. *J. Clean. Prod.* **2018**, *202*, 11−22.
(37) Rehman, F.; Ahmed, K.; Rahim, A.; Muhammad, N.; Tariq, S.; Azhar, U.; Khan, A. J.; Sama, Z.; Volpe, P. L. O.; Airoldi, C. Organo-bridged silsesquioxane incorporated mesoporous silica as a carrier for the controlled delivery of ibuprofen and fluorouracil. *J. Mol. Liq.* **2018**, *258*, 319−326.
(38) Sun, L.; Chen, Y.; Zhou, Y.; Guo, D.; Fan, Y.; Guo, F.; Zheng, Y.; Chen, W. Preparation of 5-fluorouracil-loaded chitosan nanoparticles and study of the sustained release in vitro and in vivo. *Asian J. Pharm. Sci.* **2017**, *12*, 418−423.
(39) Dardir, F. M.; Ahmed, E. A.; Soliman, M. F.; Othman, S. I.; Allam, A. A.; Alwail, M. A.; Abukhadra, M. R. Synthesis of chitosan/Al-MCM-41 nanocomposite from natural microcline as a carrier for levofloxacin drug of controlled loading and release properties; Equilibrium, release kinetic, and cytotoxicityPhysicochemical and Engineering Aspects. *Colloids Surf., A* **2021**, *624*, 126805.
(40) Baishya, H.; Gouda, R.; Qing, Z. Application of mathematical models in drug release kinetics of carbidopa and levodopa ER tablets. *J. Dev. Drugs* **2017**, *6*, 1000171.
(41) Goscianska, J.; Olejnik, A.; Nowak, I.; Marciniak, M.; Pietrzak, R. Ordered mesoporous silica modified with lanthanum for ibuprofen loading and release behaviour. *Eur. J. Pharm. Biopharm.* **2015**, *94*, 550−558.
(42) Ge, M.; Tang, W.; Du, M.; Liang, G.; Hu, G.; Alam, S. J. Research on 5-fluorouracil as a drug carrier materials with its in vitro release properties on organic modified magadiite. *Eur. J. Pharm. Sci.* **2019**, *130*, 44−53.
(43) Lin, F. H.; Lee, Y. H.; Jian, C. H.; Wong, J.-M.; Shieh, M.-J.; Wang, C.-Y. A study of purified montmorillonite intercalated with 5-fluorouracil as drug carrier. *Biomaterials* **2002**, *23*, 1981−1987.
(44) Datt, A.; Burns, E. A.; Dhuna, N. A.; Larsen, S. C. Loading and release of 5-fluorouracil from HY zeolites with varying SiO_2/Al_2O_3 ratios. *Microporous Mesoporous Mater.* **2013**, *167*, 182−187.
(45) Wang, G.; Lu, X.; Qiu, J.; Chen, P.; Chinese, J. Preparation and release performance of fluorouracil/montmorillonite complexes. *J. Chin. Ceram. Soc.* **2010**, *38*, 678−683.
(46) Wang, G.; Lu, X.; Qiu, J.; Chen, P.; Chinese, J. Preparation and release performance of fluorouracil/montmorillonite complexes. *J. Chin. Ceram. Soc.* **2010**, *38*, 678−683.

https://doi.org/10.1021/acsomega.1c06671
ACS Omega 2022, 7, 6991−7001